Published in final edited form as:
Biochemistry. 2011 April 19; 50(15): 3193–3203. doi:10.1021/bi200037j.

Coupling Efficiency of Rhodopsin and Transducin in Bicelles

Ali I. Kaya[1], **Tarjani M. Thaker**[2], **Anita M. Preininger**[1], **T. M. Iverson**[1,2,*,‡], and **Heidi E. Hamm**[1,*]

[1] Department of Pharmacology, Vanderbilt University Medical Center, Nashville, TN 37232-6600

[2] Department of Biochemistry, Vanderbilt University Medical Center, Nashville, TN 37232-6600

Abstract

G protein coupled receptors (GPCRs) can be activated by various extracellular stimuli, including hormones, peptides, odorants, neurotransmitters, nucleotides or light. After activation, activated receptors interact with heterotrimeric G proteins and catalyze GDP release from the Gα subunit, the rate limiting step in G protein activation, to form a high affinity nucleotide-free GPCR-G protein complex. *In vivo*, subsequent GTP binding reduces affinity of the Gα protein for the activated receptor. In this study, we investigated the biochemical and structural characteristics of the prototypical GPCR, rhodopsin, and its signaling partner, transducin (G_t), in phospholipid bilayers to better understand the effects of membrane composition on high affinity complex formation, stability, and receptor mediated nucleotide release. Our results demonstrate that the high-affinity complex (rhodopsin-G_t(empty)) forms more readily and has dramatically increased stability when rhodopsin is integrated into bicelles of a defined composition. We increased the half life of functional complex to one week in the presence of negatively charged phospholipids. These data suggest that a membrane-like structure is an important contributor to the formation and stability of functional receptor-G protein complexes, and can extend the range of studies that investigate properties of these complexes.

Transient complexes between integral membrane receptors and their signaling partners mediate cellular responses to disparate signals and are of high biological importance. However, these complexes are challenging to study with *in vitro* biochemical methods, since purified receptors in detergent often have both reduced functional competence and lower affinity for their binding partners, as compared to receptors in native membranes. To help develop tools for the stabilization of membrane proteins with soluble signaling partners, we selected the GPCR rhodopsin and cognate G protein G_t as a model system. These proteins provide an ideal system for monitoring complex stability, since complex formation can be monitored spectrophotometrically.

Rhodopsin is highly enriched in the rod outer segment (ROS) membranes of the retina and is responsible for low-light vision. Rhodopsin itself consists of the apoprotein (opsin) and the chromophore, 11-cis-retinal, which binds to Lys^{296} and acts as an inverse agonist (1). Absorption of a single photon photoisomerizes 11-cis-retinal to all *trans*- retinal (ATR), which is an agonist for rhodopsin. Subsequent conformational changes within rhodopsin are associated with conversion to the metarhodopsin II (MII) state, which is evidenced by a shift

*To whom correspondence should be addressed. HEH: fax, (615) 343-1084; phone, (615) 343-3533; heidi.hamm@vanderbilt.edu; TMI: fax, (615) 343-6532; phone, (615) 322-7817; tina.iverson@vanderbilt.edu.
‡Co-contributing author

†This work was supported by NIH grant EY006062 to (HEH), and NIH grants GM081816 (TMI), GM0956633 (TMI), and EY018435 (TMI), NARSAD grant 30652 (TMI), and pilot award from the Vanderbilt Institute For Chemical Biology to (TMI).

SUPPORTING INFORMATION AVAILABLE Figure S1, S2 and Table S1-S4 are available free of charge at http://pubs.acs.org.

in the wavelength of maximum absorbance by rhodopsin from 500 nm to 380 nm (2, 3). MII binds to the GDP-bound form of cognate heterotrimeric G protein, transducin (G_t-GDP), and catalyzes the release of GDP from the $G\alpha_t$ subunit, which is the rate-determining step of the G protein signaling cycle. In this high-affinity, rhodopsin-G_t(empty) complex, the activated receptor is thought to stabilize the nucleotide-free form of the Gα subunit, which, in turn, stabilizes the agonist-activated, MII form of rhodopsin. As a result, spectrophotometric monitoring of the MII signal can be used to measure formation of the catalytically competent rhodopsin-G_t(empty) complex.

Previous studies indicated that pH, temperature (4, 5), and the presence of phospholipids (6–8) all influence the formation of the rhodopsin-G_t complex. Despite known dependence upon phospholipids, many biochemical assays investigating complex formation and G protein activation are conducted in detergent micelles that are relatively poor membrane substitutes for studying receptor signaling. Furthermore, the rhodopsin and G_t interaction is significantly disturbed when detergent solubilized rhodopsin is used in functional assays (7–9). Detergent micelles and native membranes differ in many of their physical properties including packing, curvature and charge distribution. Any of these factors may result in the observed decrease in G_t affinity for detergent-solubilized rhodopsin as compared to rhodopsin in rod outer segment membranes. Interestingly, the addition of phospholipids or fatty acids (phosphatidylcholine, phosphatidylserine, phosphatidylethanolamine or docosahexaenoic acid) to detergent solubilized rhodopsin has been shown to increase the stability and protein-protein interaction capability of rhodopsin (7, 10–12). While mixing exogenous phospholipids with detergent solubilized rhodopsin has improved protein-protein interactions, the physical and structural properties of phospholipid-containing micelles are heterogeneous, making the contributions from the above factors difficult to interpret.

A number of artificial membrane models (13–18) might be used to investigate the underlying mechanism by which native membranes stabilize the rhodopsin-G_t(empty) complex. Bicelles offer distinct advantages over other artificial membrane models since they can be easily manipulated in solution and compared to other phospholipid bilayer systems such as nanodiscs, bicelles are easily prepared with a high yield. Additionally, bicelles do not interfere with the majority of biophysical measurements, and have been shown to increase the stability of purified GPCRs as compared to receptors solubilized in detergent (13). Furthermore, in the last decade, bicelles have been successfully used in crystallization, resulting in structures for bacteriorhodopsin (14), the β_2-adrenergic receptor (15), xanthorhodopsin (16) and the mouse voltage dependent anion channel (17).

Bicelle morphology (Figure 1) is hallmarked by a disc-like bilayer composed of long chain phospholipids that are capped by either short chain phospholipids or detergents (19). While bicelle structure is highly dependent on lipid composition, temperature, pH and hydration, their biochemical properties can be influenced by phospholipid-specific differences in chain lengths, saturation, and head groups (19–22). Previous studies have shown that negatively charged phospholipids such as DMPS, DMPG or DMPA can be mixed with neutral phospholipids to prepare negatively charged bicelles (22–25), which are useful for studying the effect of negatively charged phospholipids on the activity of membrane proteins. In this study, we used bicelles to investigate the effects of membrane morphology, temperature, pH, and surface charge density on the rhodopsin-G_t(empty) complex. Our results demonstrate that charge density of the bilayer is important for the formation and stability of the high affinity complex.

MATERIALS AND METHODS

Materials

HTAC; Fluka 52366, DDM; Anatrace D310, LDAO; Anatrace D360, Concanavalin A column; GE HealthScience 28-9520-85, α-methyl-D-mannopyranoside; Sigma M6882, Superdex 200 10/300 GL column; GE Healthcare 17-5174-01, DMPC, DMPA, DMPG or DMPS and the detergents DHPC, CHAPS and CHAPSO purchased from Avanti Polar Lipids.

Preparation of urea washed ROS membranes

Under dim red light conditions, ROS membranes were stripped with 7 M urea as described (26). Briefly, ROS membranes were washed twice with EDTA buffer (10 mM Tris-HCl, 1 mM EDTA, 1 mM DTT, pH 7.5) and once with urea buffer (10 mM Tris, 1 mM EDTA, 1 mM DTT, 7 M Urea, pH 7.5). After the final wash, the membranes were resuspended in buffer A (10 mM MOPS, 200 mM NaCl, 2 mM $MgCl_2$, 1 mM DTT, 100 μM PMSF, pH 7.5) and aliquot stored at −80 °C.

Purification of rhodopsin

Urea washed ROS membranes were solubilized in 50 mM Tris-HCl (pH 7.5) containing 100 mM NaCl and 20 mM DDM or 1% LDAO at 4 °C for 45 min. Insoluble material was removed by centrifugation at 20,000 × g for 1 hour at 4 °C. Detergent solubilized rhodopsin was purified by using Concanavalin-A chromatography as described (27). Briefly, the Concanavalin-A column was equilibrated with binding buffer (20 mM Tris-HCl, pH 7.4, 1 mM $MgCl_2$, 1 mM $CaCl_2$, 1 mM $MnCl_2$, 250 mM NaCl, 1 mM DTT, 0.5 mM DDM) for 48 hours at a flow rate 0.3 ml/min. Detergent solubilized rhodopsin was loaded onto the column in a continuous loop for 4 hours. The column was then washed with binding buffer (10 column volumes) and bound protein was eluted with 20 mM Tris-HCl, pH 7.4, 100 mM NaCl, 500 mM methyl α-D-mannoside and 0.5 mM DDM. Rhodopsin was concentrated using a 10 kDa cutoff concentrator and concentration of rhodopsin was determined by measuring the absorbance of rhodopsin at 500 nm before and after photo-bleaching. Molar extinction coefficients of detergent solubilized rhodopsin and rhodopsin in ROS membrane were taken as 40,600 M^{-1} cm^{-1} and 42,000 M^{-1} cm^{-1}, respectively.

Transducin purification

G_t, was prepared as previously described (28). Briefly, ROS membranes were washed four times with isotonic buffer (5 mM Tris-HCl, 130 mM KCl, 0.6 mM $MgCl_2$, 1mM EDTA, 1 mM DTT, pH 8.0) and two times with hypotonic buffer (5 mM Tris-HCl, 0.6 mM $MgCl_2$, 1mM EDTA, 1 mM DTT, pH 8.0). Membrane pellets were then washed twice with hypotonic buffer containing 0.1 mM GTP to release G_t from the membrane. Membranes were pelleted by centrifugation and the supernatant concentrated with a 10 kDa cutoff concentrator. Protein samples were dialyzed against a 20 mM Tris-HCl, pH 7.5, buffer containing 0.2 M NaCl, 10 μM GDP, 5 mM β-mercaptoethanol, 10% glycerol. Protein purity was assayed by SDS-PAGE, and protein concentration determined by Bradford assay (29).

Nucleotide Exchange Assay

Basal nucleotide exchange was determined by monitoring the intrinsic fluorescence (λ_{ex}: 300nm, λ_{em}: 340 nm) of 500 nM G_t in 10 mM MOPS buffer containing 130 mM NaCl, 1 mM $MgCl_2$ pH 7.2 for 40 min at 15 °C after addition of 10 μM GTPγS (30). Receptor mediated nucleotide exchange was determined in the presence of 500 nM light activated rhodopsin with and without addition of the indicated bicelle mixture. For bicelle

experiments, dark rhodopsin was incubated with bicelles in a lipid:protein ratio of 64000:1 on ice for 45 min. before addition of G_t.

Extra Metarhodopsin II stabilization and decay assay

Stabilization of extra MII was assessed as described (28). Briefly, 10 μM urea washed ROS membranes (or detergent solubilized rhodopsin) were incubated on ice for 15 minutes with 10 μM G_t. For bicelle experiments, detergent solubilized rhodopsin was incubated with the indicated bicelles in lipid:protein ratios ranging from 1600:1 to 12800:1 (1–8% final phospholipid concentrations) on ice for 45 min, followed by addition of varying amounts of G_t. Absorbance by rhodopsin-G protein complexes was scanned from 350 to 650 nm both before and after light activation in 50 mM HEPES (at the indicated pH) containing 0.1 M NaCl, 1mM $MgCl_2$, and 1mM DTT. In this assay, an initial dark-adapted spectrum was measured. Rhodopsin was then activated with a flash of light (activating only 10–15% of the rhodopsin). One minute after light activation a second, light adapted spectrum was collected. Rhodopsin absorption at 390 nm normalized to absorption data collected at 440 nm (the isosbestic point) was used to quantify MII formation. The extra MII signal was calculated as the difference between ΔA_{390} (light - dark) and ΔA_{440} (light - dark) (28, 31–35). For determination of extra MII decay, dark adapted 10 μM rhodopsin was incubated on ice for 15 minutes with 10 μM G_t (at this concentration over 90% of rhosdopsin was coupled with G_t according to our assay system). Then, the protein sample was completely photobleached for 10 minutes under ambient light. Spectra for the bleached samples were measured every 20 minutes over a course of 6 hours, and then again after 24 and 48 hours. After 48 hours, HCl was added to a final concentration of 260 mM to protonate the retinal Schiff base in rhodopsin and liberate free retinal (28). The half lives of the samples were calculated by fitting data to an exponential decay equation using GraphPad Prism v. 4.03 (GraphPad Software, San Diego, California).

Bicelle preparation

Bicelles composed of saturated, long-chain (14:0) DMPC, DMPA, DMPG or DMPS and the detergents (6:0) DHPC, CHAPS, or CHAPSO were prepared as a 35% stock solution with a 2.8:1 lipid to detergent ratio (q ratio) using a procedure modified from (36). Neutral bicelles were composed of DMPC and DHPC, CHAPS, or CHAPSO to form DMPC:DHPC, DMPC:CHAPS, or DMPC:CHAPSO bicelles. Negatively charged bicelles were prepared by substituting a percentage of the total molar lipid content of the neutral bicelles with negatively charged DMPA, DMPG, or DMPS, while maintaining an overall 2.8:1 phospholipid to detergent ratio. The ratio of neutral to negatively charged phospholipids is indicated within the parentheses in Figure 1. A custom extrusion apparatus was used for mixing bicelles. The apparatus was constructed by connecting two 1 mL glass syringes with tubing capped with luer locks. To prepare a 1mL, 35% stock of DMPC:DHPC bicelles, 282.50 mg DMPC was added to one syringe. 337.50 μL of a 20% DHPC solution was mixed with 312.50 μL of water. 200 μL of the DHPC solution was then added to the syringe containing DMPC. The remaining DHPC solution was added to the other syringe. The bicelle mixtures were cycled through their phase transitions 4 times by incubating the entire apparatus at 4 °C and 55 °C. Bicelles were homogenized by extrusion after each incubation. Homogeneous bicelles were transferred into a microcentrifuge tube and centrifuged at 10,000 × g for 1 minute to remove excess air bubbles. Correctly formed bicelles appeared clear at 4 °C and were stored at −20 °C. See Figure 1 for detailed information on the compositions prepared.

Dynamic Light Scattering

Dynamic light scattering measurements were collected at ambient temperatures (18–22 °C) using a DynaPro instrument (Protein Solutions, Inc). DDM detergent micelles, neutral

bicelles, and negatively charged bicelles were prepared in a buffer containing 50 mM HEPES pH 8.0, 100 mM NaCl, and 1 mM $MgCl_2$. A 2 mg/mL Conalbumin protein standard was prepared in 50 mM HEPES pH 7.4. Scattering data reported are the averages of at least 25 scans with 3 independent experiments on 60 μL samples. Data were analyzed by Dynamics V5 software (Protein Solutions, Inc) and molecular translational diffusion coefficients, D_T, were calculated by fitting the data to an exponential autocorrelation function generated by Dynamics V5. The hydrodynamic radius, R_h, was then calculated as a function of the experimental D_T using the equation $D_T = kT/6\pi\eta R_h$, where k is the Boltzmann constant, T is the experimental temperature, and η is the solvent viscosity. R_h was calculated under the assumption that scattering particles conform to diffusion properties observed for globular proteins undergoing Brownian motion in an aqueous saline solution.

Data Analysis

Graphs and statistical analysis were performed using GraphPad Prism version 4.03 (GraphPad Software, San Diego, California).

RESULTS

Formation of the rhodopsin-G_t(empty) complex in detergent

While the formation of the rhodopsin-G_t(empty) complex in ROS membranes is relatively efficient, multiple groups have demonstrated a dramatically decreased yield of the complex when G_t is mixed with purified, detergent-solubilized rhodopsin (9, 13, 37). This result was recapitulated here with DDM. In our experimental setup, we took advantage of the ability of bound G_t to stabilize the activated MII state of rhodopsin, and monitored formation of the high affinity rhodopsin-G_t(empty) complex spectrophotometrically using the extra MII assay. As anticipated, we observed that the extra MII signal for DDM-solubilized rhodopsin was only 20.7 ± 1.2 % of the maximum signal observed for complex formation in ROS membranes (Figure 2), confirming the literature reports of inefficient complex formation in detergent (9, 13, 37).

Formation of the rhodopsin-G_t(empty) complex in bicelles

Recent evidence supports a chemical role for phospholipids in formation of the rhodopsin-G_t(empty) complex (7, 9); however, the influence of geometric constraints of the membrane bilayer has not previously been addressed. Unlike spherical micelles, bicelles mimic the morphology of phospholipid membranes [(Figure 1); (38, 39)], and thus represent a suitable model system for testing the dependence of rhodopsin-G_t(empty) complex formation on membrane structure.

Our first experiments used well-defined neutral bicelles composed of DMPC:DHPC, DMPC:CHAPS, and DMPC:CHAPSO at a final concentration of 8% (w/v) (21, 24, 38, 40). In the presence of all three bicelle compositions, the observed extra MII signal from the rhodopsin-G_t(empty) complex was greater than it was in DDM (Figure 2) and reached at least 43.4 ± 7.3 % of the maximum signal observed for complex formation in ROS membranes.

ROS membranes contain both phosphatidylcholine (PC) and phosphatidylserine (PS) in a concentration of ~45% and ~15%, respectively (41–43). To assess the contribution of phosphatidylserine phospholipids to rhodopsin-G_t(empty) complex formation, we prepared bicelles doped with DMPS and capped by DHPC. In the initial trials, the molar ratio of DMPC to DMPS was fixed at 97:3 (PS (97:3) bicelles). In the presence of 8% PS (97:3) bicelles, the extra MII signal was 73.4% ± 15.6% of the extra MII signal observed in ROS membranes, essentially the same as that observed in the presence of DMPC:DHPC bicelles.

To test the effect of phosphatidylserine percentage in the bicelles on rhodopsin-G_t(empty) complex formation, the ratio of DMPS to DMPC was increased such that the DMPC:DMPS ratios were 70:**30** (PS (70:30) bicelles) and 50:**50** [(PS (50:50) bicelles, Figure 1)]. This further increased the yield of extra MII signal (Figure 3A) as compared to DDM-solubilized rhodopsin, resulting in 79.5% ± 5.2% of the ROS membrane signal in the PS (70:30) bicelles, and 87.4% ± 10.5% of the ROS membrane signal in the PS (50:50) bicelles. These data suggest that the concentration of PS indeed contributes to formation of functional rhodopsin-G_t(empty) complexes (Figure 3A).

Phosphatidylserine contains specific fatty acids and a negative charge associated with the head group. In GPCR signaling, non-specific electrostatic interactions between peripherally bound G proteins and the cell membrane influence the ability of the G protein to target to the membrane and guide its orientation on the membrane surface such that it is poised to interact with receptor (44–46). To deconvolute the contribution of chemical structure and negative charge that PS confers to the stabilization of the rhodopsin-G_t(empty) complex, we used bicelles doped with negative charges from phosphatidic acid (PA). Although PA isn't an abundant component of ROS membranes, it is important for regulation and regeneration of 11-cis retinal (47) and in the photo-transduction pathway as a precursor in the regulation of diacylglycerol and phosphatidylinositol (48, 49). The formation of the rhodopsin-G_t(empty) complex in 8% PA (97:3) bicelles was similar to that found in the presence of 8% PS (97:3) bicelles, and it wasn't significantly different from that measured in the presence of neutral bicelles. Similar to PS (70:30) bicelles, complex formation in the presence of 8% PA (70:30) was also improved, increasing complex formation to 85.9% ± 4% of that measured for ROS (Figure 3B). This suggests that the negative charge of the surface of the membrane bilayer is of greater importance to the stabilization of rhodopsin-G_t(empty) complex than any specific chemical component. The phase transition properties of PA (50:50) and all bicelles doped with the negatively-charged phosphatidylglycerol precluded detection of extra MII formation because of difficulties in sample handling.

Rhodopsin activation is also dependent on the receptor:lipid ratio (50–52). We evaluated the limiting concentration of total lipid, as well as the ratio of neutral to negatively charged lipids, required to stabilize extra MII formation. We decreased the concentrations of PS (70:30), PA (70:30), and PS (50:50) bicelles from 8% to 4%, and phospholipids were reduced from 2% to 1%, and we then assessed their ability to stabilize extra MII formation. The change in extra MII signal in the presence of decreasing total concentrations of PS (70:30), PS (50:50), and PA (70:30) phospholipids was not statistically significant between 8% and 1% (Figure 4A). This suggests that total phospholipid concentration is not a determinant of rhodopsin-G_t(empty) complex formation in the context of our assay.

To test the effect of different head groups in the negatively charged bicelle preparations on rhodopsin-G_t(empty) complex formation, PA and PS bicelles were mixed together to form a composition containing both PA and PS in the bicelle bilayer. The final concentration of negatively charged bicelles was 8% (4% PA + 4% PS bicelles). The yield of extra MII signal was further increased. We observed 94.3% ± 3.76 % of the ROS membrane signal in the presence of PA + PS (70:30) bicelles and 96.4% ± 3.50 % of the ROS membrane signal in the presence PA + PS (60:40). While not statistically significant, there was nevertheless a trend towards greater extra MII formation using a combination of PA and PS in bicelles, compared to bicelle preparations containing either PA or PS (Figure 4B).

Characterization of negatively charged bicelles by dynamic light scattering

Since not much is known regarding the morphology of bicelles containing negatively charged lipids, we verified that the addition of the negatively charged lipids did not disrupt bicelle formation using dynamic light scattering techniques. In neutral bicelles, dynamic

light scattering experiments (20, 53, 54), NMR (19, 20, 38, 53) and atomic force microscopy (20) have been used to characterize bilayer properties. Hydrodynamic radii have been determined for DMPC:DHPC bicelles, and NMR studies have confirmed that their morphology exhibits a disc-like planar bilayer at concentrations of 3% and higher (38, 53, 55), while concentrations of DMPC:DHPC below 3% may be more indicative of a vesicular morphology (38). The presence of charged phospholipids has been shown to directly affect the physical properties of phospholipid membranes, but their effects on bicelle morphology and size are largely unknown (56, 57). Dynamic light scattering (DLS) was performed to determine the homogeneity and molecular size of negatively charged bicelles compared to neutral bicelles (Figure 5). All DLS measurements were performed between 18–22 °C. Although data collection at temperatures used in the functional experiments performed in this study (4 °C and 15 °C) would have been ideal, technical limitations restricted these measurements to ambient temperatures. The calculated hydrodynamic radii derived from translational diffusion coefficients for scattering detergent micelles (54) and DMPC:DHPC bicelles were comparable to those previously reported (Figure 5) (53, 55). Compared to neutral bicelles, negatively charged bicelles exhibited larger hydrodynamic radii in solution (Table S1). The hydrodynamic radii of 8% PA (70:30), PS (70:30), and PS (50:50) bicelles were determined to be 5.7 ± 0.1 nm, 5.4 ± 0.1 nm, and 5.4 ± 0.3 nm, respectively (Figure 5). Introducing heterogeneity into the negatively charged lipid content did not affect the bicelle size; 8% PA+PS (70:30), PA+PS (60:40) bicelles were determined to have hydrodynamic radii of 5.4 ± 0.1nm and 5.4 ± 0.1 nm, respectively (Figure 5). Consistent with previous studies on DMPC:DHPC bicelles (38), decreasing the bicelle concentration below 3% dramatically affected their size. The hydrodynamic radii in the presence of a total lipid concentration of 2% for neutral or negatively charged compositions were over 12 nm, a size more typically observed in large vesicles, suggesting that the lipids no longer aggregate into disc-like bicelle membranes (Table S1) at ambient temperatures required for DLS measurements. While this may not be the case at lower temperatures used in our functional studies, we nevertheless chose to focus the remainder of our studies on complex formation in the 8% bicelle system, which maintain a disk like bicelle structure according to our DLS measurements.

Affinity of the rhodopsin-G_t(empty) complex in bicelles

Having identified bicelle compositions that allow the efficiency of rhodopsin-G_t(empty) complex formation to approach that observed in ROS membranes, we next measured the affinity of this complex using the extra MII assay comparing ROS membranes, DDM detergent, and various bicelle compositions (Figure 6). Consistent with previous studies (28), the EC_{50} value of G_t for rhodopsin in ROS membranes was 0.64 ± 0.09 μM (Table S2). As anticipated, DDM-solubilized rhodopsin exhibited a significant decrease in the affinity between rhodopsin and G_t, with an increased EC_{50} value of 3.14 ± 0.05 μM (Table S2). Bicelle-solubilized rhodopsin exhibited an intermediate affinity for G_t. In the presence of either PA (70:30) or PS (70:30) bicelles, G_t had an EC_{50} value for rhodopsin of 1.08 ± 0.12 μM and 1.08 ± 0.09 μM, respectively. Increasing the negative charge density by using PS (50:50) bicelles did not alter this affinity (EC_{50} of 1.07 ± 0.07 μM). Heterogeneity of the negatively charged lipid content improved the affinity of G_t for rhodopsin, and the EC_{50} value decreased to 0.94 ± 0.05 μM in the presence of PA+PS (70:30) bicelles. However, the affinity of G_t for rhodopsin was most comparable to that measured in ROS membranes in the presence of heterogeneous PA+PS (60:40) bicelles, where the EC_{50} value was 0.79 ± 0.05 μM. This suggests that variations in both phospholipid head group and charged density of bicelles affect the affinity between rhodopsin and G_t.

The rhodopsin-G_t(empty) complex rapidly disassociates when GTP binds to the empty nucleotide binding pocket, which is observed as a decrease in the extra MII signal. As a

control for formation of functional complexes in bicelles, rhodopsin-G_t(empty) complexes from the previous experiment were incubated with excess GTPγS. As expected, a loss in the extra MII signal was observed (Figure 6, open circles), confirming that the rhodopsin-G_t complex was functional.

Half-life of the rhodopsin-G_t(empty) complex in bicelles

The half-life of rhodopsin-G_t(empty) in the presence of negatively charged bicelles was next measured as a function of extra MII decay over time and compared to the half-life of the complex in ROS membranes and DDM. The half-life of rhodopsin-G_t(empty) was 0.63 ± 0.01 days in ROS membranes versus 0.07 ± 0.01 day in DDM micelles at pH 8.2 and 4°C. This confirms that detergent solubilization not only affects the formation efficiency of rhodopsin-G_t complexes, but also their stability. A remarkable increase in the half-life of rhodopsin-G_t(empty) complexes was observed in the presence of several bicelle compositions at pH 8.2 and 4°C (Figure 7A, Table S3). PA (70:30), PS (70:30), and PS (50:50) bicelles extended the half-life to 5.4 ± 0.2, 5.8 ± 0.3 and 5.8 ± 0.3 days, respectively. The half-life of the rhodopsin-G_t(empty) complex increased further to 6.8 ± 0.3 days in PA +PS (70:30) bicelles and 7.0 ± 0.3 days for PA+PS (60:40) bicelles. This result was not surprising, because while not statistically significant, we did observe a trend towards greater extra MII formation using the mixture of negatively charged lipids, and over the time span of decay experiments, the mixture of negatively charged lipids were found to be significantly enhanced over that seen using either negatively charged lipid alone. As a control, we incubated the samples at the end of the decay experiments in GTPγS (Figure S1), confirming that rhodopsin and G_t are both functional and form a reversible complex within these bicelles. The differences observed in the affinity and stability experiments reflect differences between how these experiments are performed; while affinity assays roughly reflect EC_{50} values, stability assays are conducted using greater than EC_{90} values of G_t. Furthermore, affinity assays employ rhodopsin that is 10–15% bleached, versus 100% bleached rhodopsin used in decay assays. Nevertheless, both experiments provide important information regarding the affinity and stability of the rhodopsin-G_t(empty)complex.

Since the MII state of rhodopsin is the physiologically relevant binding partner of G_t (5), stabilization of MII is likely to improve the half-life of the rhodopsin-G_t(empty) complex. Previous studies have demonstrated that temperature and pH influence the half-life of the rhodopsin-G_t complex (4, 5, 58), perhaps reflecting changes in stability of MII and/or changes in membrane fluidity and protein dynamics. Increasing the temperature decreased the half-life of the rhodopsin-G_t(empty) complexes formed in the presence of all compositions of bicelles tested by at least 1.5-fold, as compared to results obtained at 4 °C (Figure 7B, Table S3).

The effect of bicelle concentration on the stability of rhodopsin-G_t(empty) complex was tested in the presence of both 2% phospholipids and 8% negatively charged bicelles at different temperatures. The half life of the rhodopsin-G_t(empty) complex was decreased when the concentration of phospholipids decreased from 8% to 2% (Figure S2). This result, taken together with the DLS data, suggests that that membrane structure is an important factor for rhodopsin-G_t(empty) complex stability.

The stability of rhodopsin-G_t(empty) complexes in PA+PS (70:30) bicelles was additionally tested for pH-dependence (Figure 7C). A decrease in pH from 8.2 to 6.5 at 4 °C resulted in a 1.5 fold decrease in the complex half-life. This was much longer than the half-life of the complex in ROS membranes (28), suggesting that extra MII instability at pH 6.5 is not a property of extra MII only but of the native membrane environment. While increasing the pH from 8.2 to 9.0 at 4 °C had a negligible effect on stability (Figure 7C, black bars), increasing the temperature had a more pronounced effect. Increasing the temperature from 4

to 15 °C resulted in a nearly 1.5 fold decrease in the half-life of the complex, regardless of pH value tested (Figure 7C, grey bars).

It is well established that the addition excess of ATR to rhodopsin can activate rhodopsin and stabilize the MII state (59, 60). Accordingly, we measured the half-life of rhodopsin-G_t(empty) complex in the presence of 1.5 fold molar excess of ATR in both ROS and in a negatively charged phospholipid preparation. Not surprisingly, the half life of complex increased from 0.62 ± 0.01 to 0.97 ± 0.03 days at 4 °C in presence of ROS membranes, and in our 2% PA+PS (60:40) phospholipid preparation, addition of ATR increased the half life of the complexes to 4.0 ± 0.5 days at 15 °C. Lowering the temperature to 4 °C further extended the half life to 7.2 ± 0.2 days in this lipid preparation. These data are consistent with ATR's ability to stabilize the rhodopsin-Gt(empty) complex, similar to reported effects of ATR on MII stability.

Receptor-catalyzed nucleotide exchange in the presence of bicelles

Previous studies have shown that the addition of phosphatidylcholine, phosphatidylserine or phosphatidylethanolamine exerts differential effects on receptor-catalyzed nucleotide exchange in the Gα subunit of the G protein, with G_t activation rates altered specifically by the presence of phosphatidylserine (9). To evaluate the effect of our optimized bicelle compositions on G_t function, the receptor-catalyzed nucleotide exchange rate was determined using an intrinsic tryptophan fluorescence assay (Figure 8), which reflects the ability of an activated receptor to stimulate GDP-GTP exchange on the G protein. The nucleotide exchange rates in PA (70:30), PS (70:30), or PS (50:50) bicelles were similar to those observed in ROS membranes (Table S4). Additionally, heterogeneity of negatively charged bicelles enhanced rates of G protein activation. The nucleotide exchange rate in the presence of PA+PS (70:30) and PA+PS (60:40) were measured 4.62 ± 0.30 and 4.48 ± 0.51 ($1/sec \times 10^{-2}$), respectively (Figure 8, Table S4).

DISCUSSION

Early studies on receptor-G protein coupling indicate that temperature, pH, and the presence of lipids each influence complex formation (4, 5, 7, 58), but our understanding of the contribution of membrane lipids to complex stabilization has been limited to experiments performed in detergent micelles, mixed micelles, and other undefined lipid preparations. Findings in recent years have increased our appreciation of the importance of membrane morphology and composition on receptor structure and function. Unlike spherical detergent micelles, bicelles usually adopt a disk-like shape, which NMR studies indicate are similar in morphology to native membranes (19, 38). Bicelles have also previously demonstrated an ability to support folding and thermal stability of rhodopsin and opsin (13). Here, we investigated the formation and stabilization of a receptor-G protein complex by incorporating negatively charged phospholipids into a neutral bicelle preparation.

Biochemical and biophysical studies have demonstrated that the lipid bilayer is important for the assembly, stability, and function of membrane proteins (61–63). In ROS membranes, rhodopsin is also surrounded by a specific phospholipid composition that likely facilitates visual transduction processes, and contain roughly ~2.5 % phosphatidylinositol, ~13% phosphatidylserine, ~41% phosphatidylethanolamine, ~45 % phosphatidylcholine (41–43). Since rhodopsin-G_t coupling is significantly less efficient in detergent micelles than in ROS membranes or neutral or negatively-charged bicelles, this specific lipid environment may contribute to visual signaling by optimizing the stability of this complex. Our studies confirm the previously observation that negatively charged lipids improve the efficiency of rhodopsin activation and G protein interaction (9, 64–67). We have found that the overall charge of the specific bicelles influenced formation and stability of the high affinity

receptor-G protein complex, likely through a combination of electrostatic and physical effects, as electrostatics are known to play a role in receptor-G protein interaction (44, 45). In our experiments, increasing the density of negatively charged phospholipids in bicelles enhanced the complex formation, stability, and rates of receptor-mediated G protein activation, supporting a role for electrostatics in stabilizing optimal receptor-G protein coupling (44). The physical properties of bicelles most likely stabilize the receptor-G protein complex structure better than ROS membranes through enhanced G protein docking and membrane anchoring than what is available in the native lipid environment. Here we present evidence of functional rhodopsin-G_t complexes in an artificial membrane environment that incorporates negatively charged phospholipids into a neutral bicelle.

Bicelle morphology and phase properties are extremely sensitive to changes in temperature, phospholipid concentration in solution, and q ratio. In the case of neutral bicelles, decreasing the total concentration below a critical percentage results in formation of large unilamellar vesicles (38). In terms of neutral bicelles, decreasing final concentration of bicelles or increasing q ratios and temperatures is known to induce a phase transition from disc-like bicelles to an extended network of interconnected lipids called the perforated lamellar phase, or “swiss cheese”-like phase, characterized by high sample viscosity (21, 38). Here we observed similar effects on bicelle morphology and phase properties. Hydrodynamic radii dramatically increased when the total phospholipid concentration was decreased to 2% at ambient temperatures, which suggests formation of large vesicles (38) at temperatures above those used in our functional studies. All compositions of negatively charged bicelles were temperature sensitive, and became highly viscous above 24°C, which is the phase transition temperature for DMPC (38). Interestingly, the stability of negatively charged bicelle phase, as assessed by color and fluidity, appeared to be the greatest at below 20°C.

Lipids are known to be important for optimal function of many trans-membrane proteins. Disruption of the membrane phospholipid composition during protein purification can affect the folding of membrane proteins, and consequently, signaling capabilities. For example, changes in temperature can lead to increased phospholipid dynamics and membrane fluidity, which contribute to receptor destabilization. Temperature also has observable effects on bicelle properties, as changes in temperature result in phase transitions. When the temperature is increased from 4 to 15 °C, we noted a decrease in the decay half-life of the complex in bicelles, consistent with results in other systems (4, 68). Taken together, we suggest that bicelle preparations containing negatively charged phospholipids facilitate stabilization of receptor-G protein complexes, and this effect is most evident at lower temperatures, compatible with temperatures used in most functional studies.

The metarhodopsin I/metarhodopsin II, (MI/MII) equilibrium of rhodopsin governs the productive coupling of receptor with G proteins, with coupling to MII being substantially more efficient (5). Knierim *et al.* showed that more than one proton is released from the MII state when rhodopsin binds to the C-terminal peptide of Gα (69). Sato *et al.* reached a similar conclusion using a computational approach, wherein an initial decrease in extra MII was predicted as the pH was raised, followed by an increase in extra MII at even higher pH’s. Similarly, we observe that increasing the pH from 6.2 to 8.5 in the presence of negatively charged phospholipid compositions enhances the half-life of the high affinity complex. These results suggest that negatively charged bicelles contribute to the stability of the complex by both enhancing MII formation, as well as facilitating the G protein orientation at the membrane necessary for productive interactions with receptors.

Further studies are planned to determine the effect of bicelles doped with other negatively charged phospholipids commonly found in membranes, such as phosphatidylinositols, on stability of the receptor-G protein complex. This study will include effects of varying acyl

chain length and saturation of the phospholipids, which can have effects on both receptor activation and receptor-G protein coupling (10–12, 70). While 14:0 fatty acids are not a major acyl chain constituent of lipids in ROS membranes, 14:0 lipids have been used successfully in other bicelle systems to stabilize receptor structure (14, 15, 17). The addition of cholesterol, as well as phospholipids which vary in headgroup size and charge, have also been shown to have effects on receptor-G protein interaction and G protein activation (7, 9, 71), suggesting this may be another factor requiring further study.

Summary and conclusions

A highly complex lipid environment allows the adaptability and flexibility in membrane structure required for the cellular signaling. Our data demonstrate that rhodopsin-G_t interactions and G protein activation is strongly dependent on phospholipid composition and charge density. We developed an optimized system that included PA+PS (60:40) bicelles, which increased the half-life of the rhodopsin-G_t(empty) complex to one week. This system provides a powerful tool for the study of GPCR-G protein complexes, and the fundamental approaches described here may be applicable to other complexes between membrane proteins and their soluble signaling partners.

Supplementary Material

Refer to Web version on PubMed Central for supplementary material.

Acknowledgments

We thank Dr. Charles R. Sanders and Dr. Vsevolod V. Gurevich for valuable discussions and critical reading of the manuscript. A portion of this work used facilities that were supported by P30EY008126.

ABBREVIATIONS

ATR	all *trans*- retinal
CHAPS	3-[(3-Cholamidopropyl)dimethylammonio]-1-propanesulfonate
CHAPSO	3-[(3-Cholamidopropyl)dimethylammonio]-2-hydroxy-1-propanesulfonate
DDM	n-Dodecyl-β-D-maltopyrannoside
DHPC	1,2-dihexanoyl-sn-glycero-3-phosphocholine
DMPA	1,2-dimyristoyl-sn-glycero-3-phosphate
DMPC	dimyristoyl-sn-glycero-3-phosphocholine
DMPG	1,2-dimyristoyl-sn-glycero-3-phospho-(1′-rac-glycerol)
DMPS	1,2-dimyristoyl-sn-glycero-3-phospho-L-serine
GTP	guanosine-5′-triphosphate
GTPγS	guanosine-5′-O-[gamma-thio]triphosphate
GDP	guanosine diphosphate
HTAC	Hexadecyltrimethylammonium Chloride
LDAO	n-Dodecyl-N,N-Dimethylamine-N-oxide

References

1. Okada T, Ernst OP, Palczewski K, Hofmann KP. Activation of rhodopsin: new insights from structural and biochemical studies. Trends Biochem Sci. 2001; 26:318–324. [PubMed: 11343925]
2. Palczewski K. G protein-coupled receptor rhodopsin. Annu Rev Biochem. 2006; 75:743–767. [PubMed: 16756510]
3. Emeis D, Kuhn H, Reichert J, Hofmann KP. Complex formation between metarhodopsin II and GTP-binding protein in bovine photoreceptor membranes leads to a shift of the photoproduct equilibrium. FEBS Lett. 1982; 143:29–34. [PubMed: 6288450]
4. Parkes JH, Gibson SK, Liebman PA. Temperature and pH dependence of the metarhodopsin I-metarhodopsin II equilibrium and the binding of metarhodopsin II to G protein in rod disk membranes. Biochemistry. 1999; 38:6862–6878. [PubMed: 10346908]
5. Parkes JH, Liebman PA. Temperature and pH dependence of the metarhodopsin I-metarhodopsin II kinetics and equilibria in bovine rod disk membrane suspensions. Biochemistry. 1984; 23:5054–5061. [PubMed: 6498176]
6. Fung JJ, Deupi X, Pardo L, Yao XJ, Velez-Ruiz GA, Devree BT, Sunahara RK, Kobilka BK. Ligand-regulated oligomerization of beta(2)-adrenoceptors in a model lipid bilayer. EMBO J. 2009; 28:3315–3328. [PubMed: 19763081]
7. Alves ID, Salgado GF, Salamon Z, Brown MF, Tollin G, Hruby VJ. Phosphatidylethanolamine enhances rhodopsin photoactivation and transducin binding in a solid supported lipid bilayer as determined using plasmon-waveguide resonance spectroscopy. Biophys J. 2005; 88:198–210. [PubMed: 15501933]
8. Litman BJ, Niu SL, Polozova A, Mitchell DC. The role of docosahexaenoic acid containing phospholipids in modulating G protein-coupled signaling pathways: visual transduction. J Mol Neurosci. 2001; 16:237–242. discussion 279–284. [PubMed: 11478379]
9. Jastrzebska B, Goc A, Golczak M, Palczewski K. Phospholipids are needed for the proper formation, stability, and function of the photoactivated rhodopsin-transducin complex. Biochemistry. 2009; 48:5159–5170. [PubMed: 19413332]
10. Mitchell DC, Niu SL, Litman BJ. Optimization of receptor-G protein coupling by bilayer lipid composition I: kinetics of rhodopsin-transducin binding. J Biol Chem. 2001; 276:42801–42806. [PubMed: 11544258]
11. Gawrisch K, Soubias O, Mihailescu M. Insights from biophysical studies on the role of polyunsaturated fatty acids for function of G-protein coupled membrane receptors. Prostaglandins Leukot Essent Fatty Acids. 2008; 79:131–134. [PubMed: 19004627]
12. Bennett MP, Mitchell DC. Regulation of membrane proteins by dietary lipids: effects of cholesterol and docosahexaenoic acid acyl chain-containing phospholipids on rhodopsin stability and function. Biophys J. 2008; 95:1206–1216. [PubMed: 18424497]
13. McKibbin C, Farmer NA, Jeans C, Reeves PJ, Khorana HG, Wallace BA, Edwards PC, Villa C, Booth PJ. Opsin stability and folding: modulation by phospholipid bicelles. J Mol Biol. 2007; 374:1319–1332. [PubMed: 17996895]
14. Faham S, Boulting GL, Massey EA, Yohannan S, Yang D, Bowie JU. Crystallization of bacteriorhodopsin from bicelle formulations at room temperature. Protein Sci. 2005; 14:836–840. [PubMed: 15689517]
15. Rasmussen SG, Choi HJ, Rosenbaum DM, Kobilka TS, Thian FS, Edwards PC, Burghammer M, Ratnala VR, Sanishvili R, Fischetti RF, Schertler GF, Weis WI, Kobilka BK. Crystal structure of the human beta2 adrenergic G-protein-coupled receptor. Nature. 2007; 450:383–387. [PubMed: 17952055]
16. Luecke H, Schobert B, Stagno J, Imasheva ES, Wang JM, Balashov SP, Lanyi JK. Crystallographic structure of xanthorhodopsin, the light-driven proton pump with a dual chromophore. Proc Natl Acad Sci U S A. 2008; 105:16561–16565. [PubMed: 18922772]
17. Ujwal R, Cascio D, Colletier JP, Faham S, Zhang J, Toro L, Ping P, Abramson J. The crystal structure of mouse VDAC1 at 2.3 A resolution reveals mechanistic insights into metabolite gating. Proc Natl Acad Sci U S A. 2008; 105:17742–17747. [PubMed: 18988731]

18. Bayburt TH, Vishnivetskiy SA, McLean MA, Morizumi T, Huang CC, Tesmer JJ, Ernst OP, Sligar SG, Gurevich VV. Monomeric rhodopsin is sufficient for normal rhodopsin kinase (GRK1) phosphorylation and arrestin-1 binding. J Biol Chem. 2011; 286:1420–1428. [PubMed: 20966068]
19. Sanders CR, Prosser RS. Bicelles: a model membrane system for all seasons? Structure. 1998; 6:1227–1234. [PubMed: 9782059]
20. Wu H, Su K, Guan X, Sublette ME, Stark RE. Assessing the size, stability, and utility of isotropically tumbling bicelle systems for structural biology. Biochim Biophys Acta. 2010; 1798:482–488. [PubMed: 19914202]
21. Glover KJ, Whiles JA, Wu G, Yu N, Deems R, Struppe JO, Stark RE, Komives EA, Vold RR. Structural evaluation of phospholipid bicelles for solution-state studies of membrane-associated biomolecules. Biophys J. 2001; 81:2163–2171. [PubMed: 11566787]
22. Struppe J, Whiles JA, Vold RR. Acidic phospholipid bicelles: A versatile model membrane system. Biophysical Journal. 2000; 78:281–289. [PubMed: 10620292]
23. Struppe J, Komives EA, Taylor SS, Vold RR. 2H NMR studies of a myristoylated peptide in neutral and acidic phospholipid bicelles. Biochemistry. 1998; 37:15523–15527. [PubMed: 9799515]
24. Marcotte I, Auger M. Bicelles as model membranes for solid- and solution-state NMR studies of membrane peptides and proteins. Concepts in Magnetic Resonance Part A. 2005; 24A:17–37.
25. Prosser RS, Hwang JS, Vold RR. Magnetically aligned phospholipid bilayers with positive ordering: a new model membrane system. Biophys J. 1998; 74:2405–2418. [PubMed: 9591667]
26. Mazzoni MR, Malinksi JA, Hamm HE. Structural Analysis of Rod GTP-binding Protein, G_t. Limited Proteolytic Digestion Pattern of G_t with Four Proteases Defines Monoclonal Antibody Epitope. Journal of Biological Chemistry. 1991; 266:14072–14081. [PubMed: 1713215]
27. Litman BJ. Purification of rhodopsin by concanavalin A affinity chromatography. Methods Enzymol. 1982; 81:150–153. [PubMed: 7098858]
28. Aris L, Gilchrist A, Rens-Domiano S, Meyer C, Schatz PJ, Dratz EA, Hamm HE. Structural Requirements for the Stabilization of Metarhodopsin II by the C Terminus of the α subunit of Transducin. Journal of Biological Chemistry. 2001; 276:2333–2339. [PubMed: 11018024]
29. Bradford MM. A rapid and sensitive method for the quantitation of microgram quantities of protein utilizing the principle of protein-dye binding. Anal Biochem. 1976; 72:248–254. [PubMed: 942051]
30. Preininger A, Funk M, Meier S, Oldham W, Johnston C, Adhikary S, Kimple A, Siderovski D, Hamm H, Iverson T. Helix dipole movement and conformational variability contribute to allosteric GDP release in Gi subunits. Biochemistry. 2009; 48:2630–2642. [PubMed: 19222191]
31. Schleicher A, Kuhn H, Hofmann KP. Kinetics, binding constant, and activation energy of the 48-kDa protein-rhodopsin complex by extra-metarhodopsin II. Biochemistry. 1989; 28:1770–1775. [PubMed: 2719933]
32. Hoffmann W, Siebert F, Hofmann KP, Kreutz W. Two distinct rhodopsin molecules within the disc membrane of vertebrate rod outer segments. Biochim Biophys Acta. 1978; 503:450–461. [PubMed: 28757]
33. Emeis D, Hofmann KP. Shift in the relation between flash-induced metarhodopsin I and metarhodpsin II within the first 10% rhodopsin bleaching in bovine disc membranes. FEBS Lett. 1981; 136:201–207. [PubMed: 7327258]
34. Kisselev OG, Meyer CK, Heck M, Ernst OP, Hofmann KP. Signal transfer from rhodopsin to the G-protein: evidence for a two-site sequential fit mechanism. Proc Natl Acad Sci U S A. 1999; 96:4898–4903. [PubMed: 10220390]
35. Chen Y, Herrmann R, Fishkin N, Henklein P, Nakanishi K, Ernst OP. Synthesis and spectroscopic characterization of photo-affinity peptide ligands to study rhodopsin-G protein interaction. Photochem Photobiol. 2008; 84:831–838. [PubMed: 18282180]
36. Faham S, Bowie JU. Bicelle crystallization: a new method for crystallizing membrane proteins yields a monomeric bacteriorhodopsin structure. J Mol Biol. 2002; 316:1–6. [PubMed: 11829498]
37. Bayburt TH, Leitz AJ, Xie G, Oprian DD, Sligar SG. Transducin activation by nanoscale lipid bilayers containing one and two rhodopsins. J Biol Chem. 2007; 282:14875–14881. [PubMed: 17395586]

38. Sanders CR, Schwonek JP. Characterization of Magnetically Orientable Bilayers in Mixtures of Dihexanoylphosphatidylcholine and Dimyristoylphosphatidylcholine by Solid-State Nmr. Biochemistry. 1992; 31:8898–8905. [PubMed: 1390677]
39. Sanders CR, Kuhn Hoffmann A, Gray DN, Keyes MH, Ellis CD. French swimwear for membrane proteins. Chembiochem. 2004; 5:423–426. [PubMed: 15185363]
40. Whiles JA, Deems R, Vold RR, Dennis EA. Bicelles in structure-function studies of membrane-associated proteins. Bioorg Chem. 2002; 30:431–442. [PubMed: 12642127]
41. Boesze-Battaglia K, Schimmel R. Cell membrane lipid composition and distribution: implications for cell function and lessons learned from photoreceptors and platelets. J Exp Biol. 1997; 200:2927–2936. [PubMed: 9359876]
42. Eichberg J, Hess HH. The lipid composition of frog retinal rod outer segments. Experientia. 1967; 23:993–994. [PubMed: 6077901]
43. Wiegand RD, Naash MI, Penn JS, Maude MB, Anderson RE. Effect of Constant Light on Rat Retinas Deficient in Glutathione-Reductase. Federation Proceedings. 1986; 45:1728–1728.
44. Kosloff M, Alexov E, Arshavsky VY, Honig B. Electrostatic and lipid anchor contributions to the interaction of transducin with membranes: mechanistic implications for activation and translocation. J Biol Chem. 2008; 283:31197–31207. [PubMed: 18782760]
45. Lambright DG, Sondek J, Bohm A, Skiba NP, Hamm HE, Sigler PB. The 2.0 A crystal structure of a heterotrimeric G protein. Nature. 1996; 379:311–319. [PubMed: 8552184]
46. Bohm A, Gaudet R, Sigler PB. Structural aspects of heterotrimeric G-protein signaling. Curr Opin Biotechnol. 1997; 8:480–487. [PubMed: 9265729]
47. Saari JC, Nawrot M, Stenkamp RE, Teller DC, Garwin GG. Release of 11-cis-retinal from cellular retinaldehyde-binding protein by acidic lipids. Mol Vis. 2009; 15:844–854. [PubMed: 19390642]
48. Ilincheta de Boschero MG, Giusto NM. Phosphatidic acid and polyphosphoinositide metabolism in rod outer segments. Differential role of soluble and peripheral proteins. Biochim Biophys Acta. 1992; 1127:105–115. [PubMed: 1322705]
49. LaLonde MM, Janssens H, Rosenbaum E, Choi SY, Gergen JP, Colley NJ, Stark WS, Frohman MA. Regulation of phototransduction responsiveness and retinal degeneration by a phospholipase D-generated signaling lipid. J Cell Biol. 2005; 169:471–479. [PubMed: 15883198]
50. Calvert PD, Govardovskii VI, Krasnoperova N, Anderson RE, Lem J, Makino CL. Membrane protein diffusion sets the speed of rod phototransduction. Nature. 2001; 411:90–94. [PubMed: 11333983]
51. Aveldano MI. Phospholipid solubilization during detergent extraction of rhodopsin from photoreceptor disk membranes. Arch Biochem Biophys. 1995; 324:331–343. [PubMed: 8554325]
52. Nickell S, Park PS, Baumeister W, Palczewski K. Three-dimensional architecture of murine rod outer segments determined by cryoelectron tomography. J Cell Biol. 2007; 177:917–925. [PubMed: 17535966]
53. Andersson A, Maler L. Size and shape of fast-tumbling bicelles as determined by translational diffusion. Langmuir. 2006; 22:2447–2449. [PubMed: 16519439]
54. Dupuy C, Auvray X, Petipas C. Anomeric effects on the structure of micelles of alkyl maltosides in water. Langmuir. 1997; 13:3965–3967.
55. Kozak M, Kempka M, Szpotkowski K, Jurga S. NMR in soft materials: A study of DMPC/DHPC bicellar system. J Non-Cryst Solids. 2007; 353:4246–4251.
56. Botelho AV, Huber T, Sakmar TP, Brown MF. Curvature and hydrophobic forces drive oligomerization and modulate activity of rhodopsin in membranes. Biophys J. 2006; 91:4464–4477. [PubMed: 17012328]
57. Botelho AV, Gibson NJ, Thurmond RL, Wang Y, Brown MF. Conformational energetics of rhodopsin modulated by nonlamellar-forming lipids. Biochemistry. 2002; 41:6354–6368. [PubMed: 12009897]
58. Sato K, Morizumi T, Yamashita T, Shichida Y. Direct observation of the pH-dependent equilibrium between metarhodopsins I and II and the pH-independent interaction of metarhodopsin II with transducin C-terminal peptide. Biochemistry. 2010; 49:736–741. [PubMed: 20030396]

59. Jager S, Palczewski K, Hofmann KP. Opsin/all-trans-retinal complex activates transducin by different mechanisms than photolyzed rhodopsin. Biochemistry. 1996; 35:2901–2908. [PubMed: 8608127]
60. Jastrzebska B, Golczak M, Fotiadis D, Engel A, Palczewski K. Isolation and functional characterization of a stable complex between photoactivated rhodopsin and the G protein, transducin. FASEB J. 2009; 23:371–381. [PubMed: 18827025]
61. Lee AG. Lipid-protein interactions in biological membranes: a structural perspective. Biochim Biophys Acta. 2003; 1612:1–40. [PubMed: 12729927]
62. Shogomori H, Brown DA. Use of detergents to study membrane rafts: the good, the bad, and the ugly. Biol Chem. 2003; 384:1259–1263. [PubMed: 14515986]
63. Simons K, Ikonen E. Functional rafts in cell membranes. Nature. 1997; 387:569–572. [PubMed: 9177342]
64. Gibson NJ, Brown MF. Role of phosphatidylserine in the MI-MII equilibrium of rhodopsin. Biochem Biophys Res Commun. 1991; 176:915–921. [PubMed: 2025300]
65. Gibson NJ, Brown MF. Lipid headgroup and acyl chain composition modulate the MI-MII equilibrium of rhodopsin in recombinant membranes. Biochemistry. 1993; 32:2438–2454. [PubMed: 8443184]
66. Bayburt TH, Vishnivetskiy SA, McLean MA, Morizumi T, Huang CC, Tesmer JJ, Ernst OP, Sligar SG, Gurevich VV. Monomeric rhodopsin is sufficient for normal rhodopsin kinase (GRK1) phosphorylation and arrestin-1 binding. J Biol Chem. 2010
67. Tsukamoto H, Sinha A, DeWitt M, Farrens DL. Monomeric rhodopsin is the minimal functional unit required for arrestin binding. J Mol Biol. 2010; 399:501–511. [PubMed: 20417217]
68. Kohl B, Hofmann KP. Temperature dependence of G-protein activation in photoreceptor membranes. Transient extra metarhodopsin II on bovine disk membranes. Biophys J. 1987; 52:271–277. [PubMed: 3117126]
69. Knierim B, Hofmann KP, Ernst OP, Hubbell WL. Sequence of late molecular events in the activation of rhodopsin. Proc Natl Acad Sci U S A. 2007; 104:20290–20295. [PubMed: 18077356]
70. Feller SE. Acyl chain conformations in phospholipid bilayers: a comparative study of docosahexaenoic acid and saturated fatty acids. Chem Phys Lipids. 2008; 153:76–80. [PubMed: 18358239]
71. Niu SL, Mitchell DC, Litman BJ. Optimization of receptor-G protein coupling by bilayer lipid composition II: formation of metarhodopsin II-transducin complex. J Biol Chem. 2001; 276:42807–42811. [PubMed: 11544259]

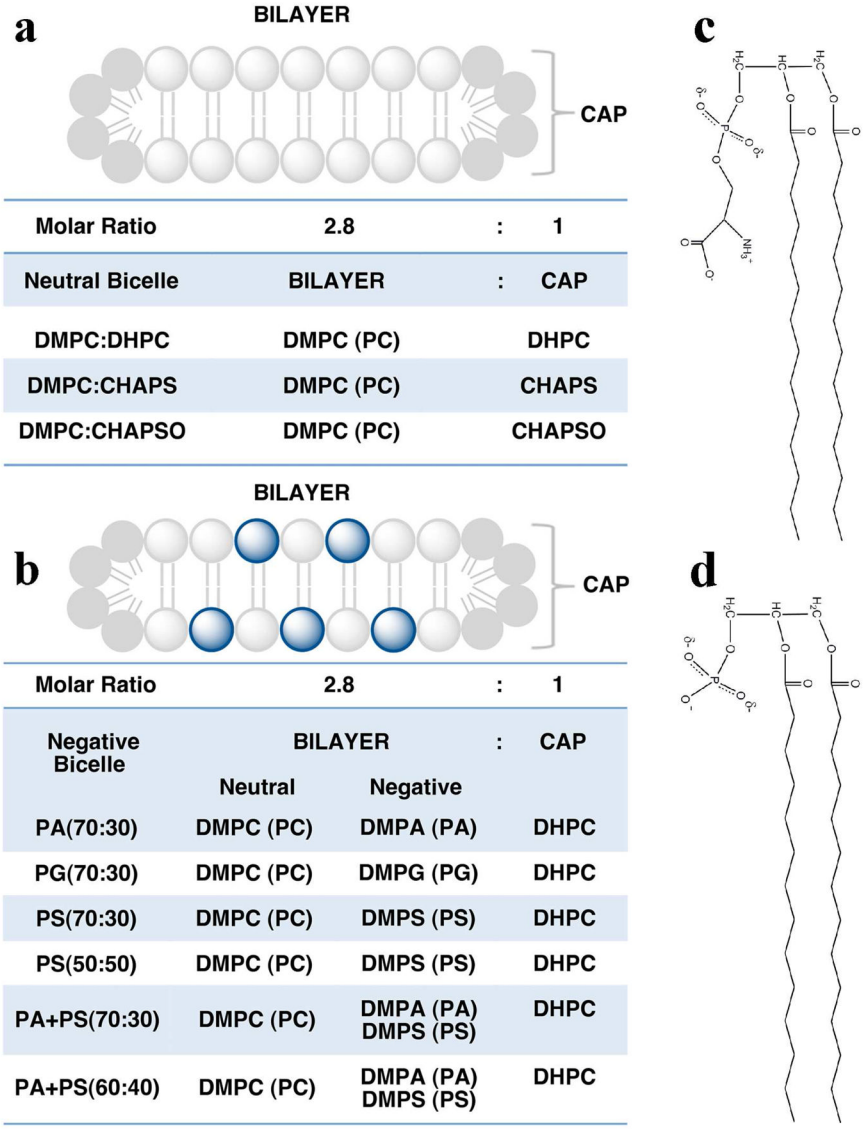

Figure 1.

Bicelle morphology and composition. Bicelles are disc-like membrane structures composed of long-chain phospholipids and capped by either detergents or short-chained phospholipids. The radius of the disc is dependent on the long-chain phospholipid to detergent or short-chain phospholipid molar ratio (q ratio). The width of the bilayer is dependent on the acyl-chain length of the long-chain phospholipid. In this study, all bicelles compositions were prepared in a 2.8:1 phospholipid:detergent molar ratio with 14:0 phospholipids comprising the bilayer. (**a**) Neutral bicelles were composed of DMPC bilayers capped with 6:0 DHPC, CHAPS, or CHAPSO. (**b**) Negatively charged bicelles were composed of 14:0 phospholipids mixed with DHPC (6:0) in a 2.8:1 ratio. The ratio of neutral to negatively charged phospholipids is indicated within the parentheses in the graph. Schematic representation of (**c**) DMPS and (**d**) DMPA phospholipids.

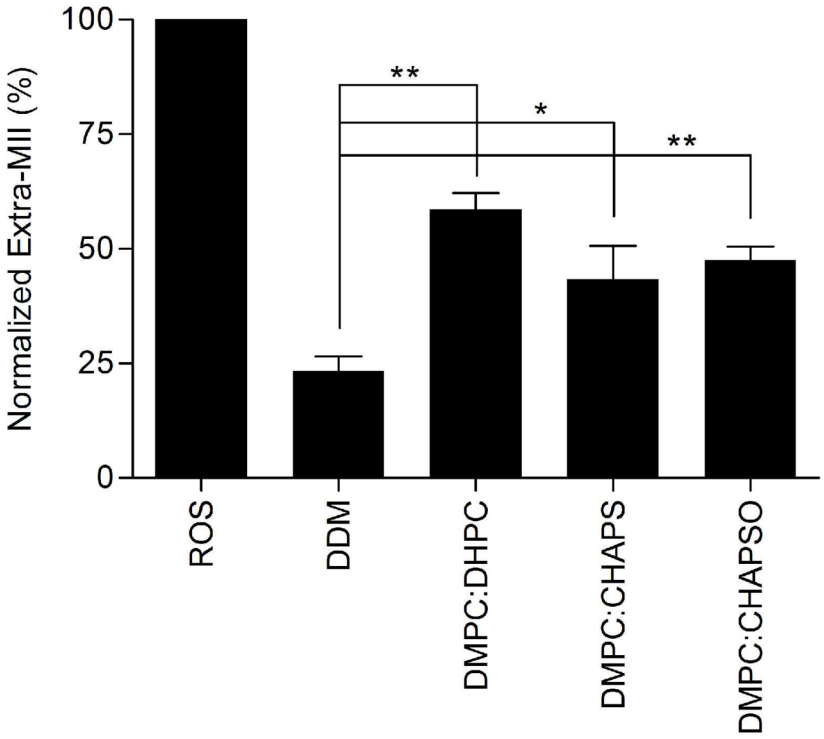

Figure 2.

Neutral bicelles support extra MII stabilization. Normalized quantitation of extra metarhodopsin II in the absence or presence of neutral bicelles. The final concentration of bicelles was 8 %. Data were obtained at 4 °C and normalized to the extra-metarhodopsin signal measured in ROS membranes under the same conditions. Results are mean ± S.E.M. of three independent experiments (* $p < 0.05$; ** $p < 0.01$).

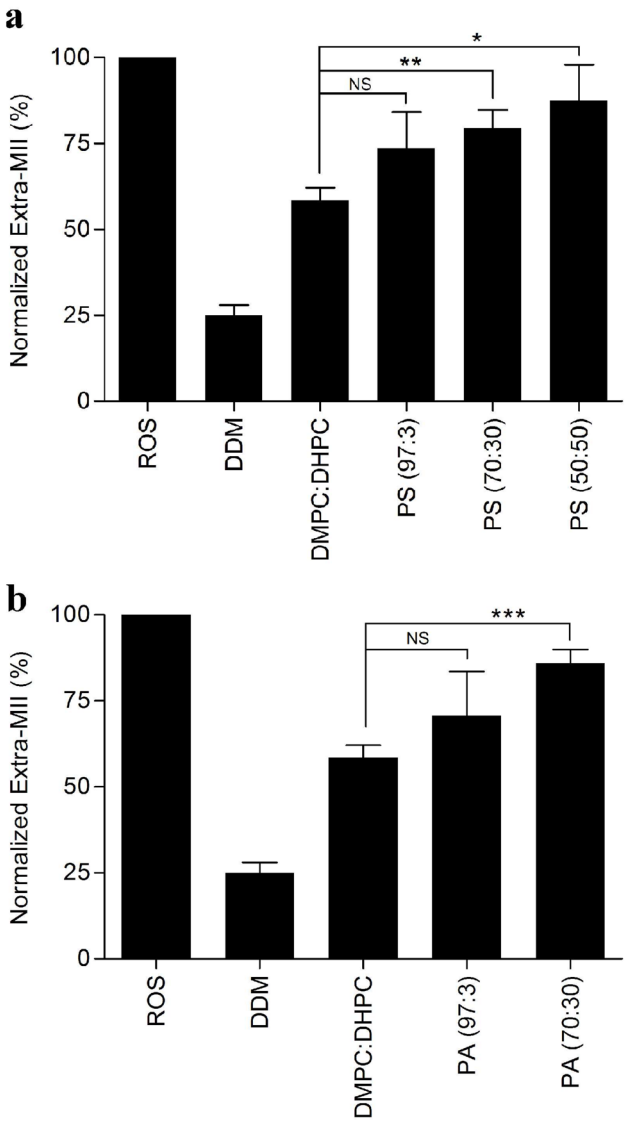

Figure 3.

Anionic lipid enhances extra MII stabilization. Quantiation of extra-metarhodopsin II in the presence of different negatively charged bicelles. Extra-metarhodopsin II was assessed in the presence of (**a**) DMPS or (**b**) DMPA containing bicelles. The ratio of neutral to negatively charged phospholipids, DMPC:DMPS (or DMPA), was 97:3, 70:30 or 50:50 in these bicelles. The final concentration of bicelles was 8%. The average lipid:rhodopsin ratio was 12800:1. Data were collected at 4 °C and normalized to the extra-metarhodopsin signal measured in ROS membranes under the same conditions. Results are mean ± S.E.M. values of three independent experiments (* $p < 0.05$; ** $p < 0.01$; *** $p < 0.001$; NS, Not Significant).

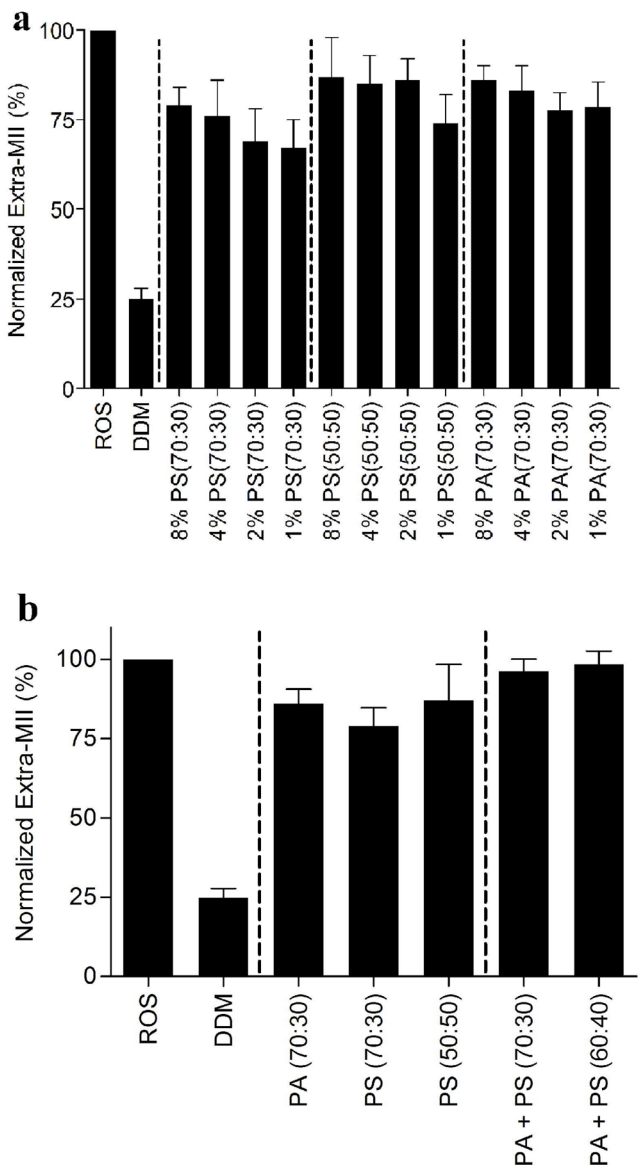

Figure 4.

Complex mixtures of anionic lipids in bicelle preparations. The effect of bicelle concentration on rhodopsin-G_t(empty) formation. (**a**) The effect of varying concentrations of PS (70:30), PS (50:50) and PA (70:30) bicelles on rhodopsin-G_t(empty) complex formation. Final concentration of bicelles was decreased from 8% to 4% and phospholipids concentration decreased from 2% to 1% (with lipid:rhodopsin ratios of 12800:1 to 1600:1) as indicated in the graph. (**b**) The effect of mixing PA and PS bicelles on rhodopsin-G_t(empty) formation. The final concentration of negatively charged bicelles was 8% (4% PA + 4% PS bicelles). The average lipid:rhodopsin ratio was 12800:1. The ratio of neutral to negatively charged phospholipids is indicated within parentheses in the graph. Data were collected at 4 °C and normalized to the extra-metarhodopsin signal measured in ROS membranes under the same conditions. Results are mean ± S.E.M. values of three independent experiments.

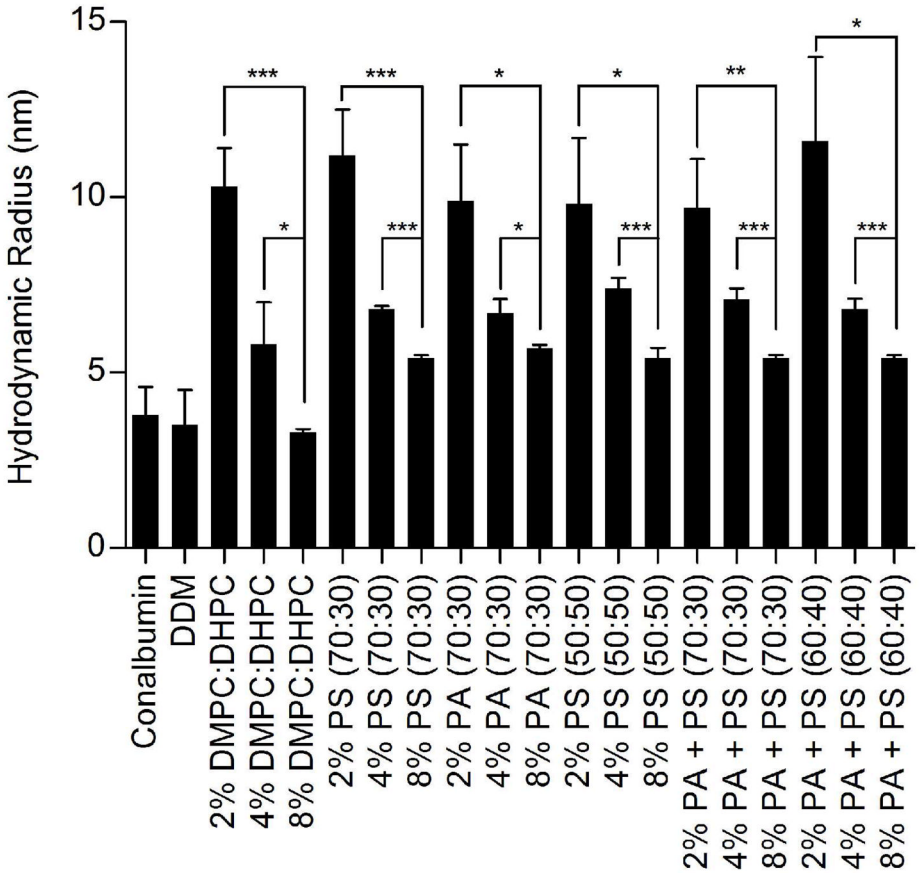

Figure 5.

Dynamic Light Scattering measurements on negatively charged bicelles. Data was collected on samples at final phospholipid concentrations of 2%, 4%, and 8% in solution. All samples were prepared in extra MII assay buffer (50 mM HEPES pH 8.0, 100 mM NaCl, 1 mM $MgCl_2$). 2 mg/mL Conalbumin (75 kDa) and 0.5 mM DDM (70 kDa) were prepared as positive controls. Hydrodynamic radii were determined by Dynamics V5 software, with light scattering data collected at 18–22°C on a DynaPro detector. The ratio of neutral to negatively charged phospholipids is indicated within the parentheses in the graph. Results are are means ± S.E.M. of at least 25 scans with two independent experiments (* $p < 0.05$; ** $p < 0.01$; *** $p < 0.001$; NS, Not Significant).

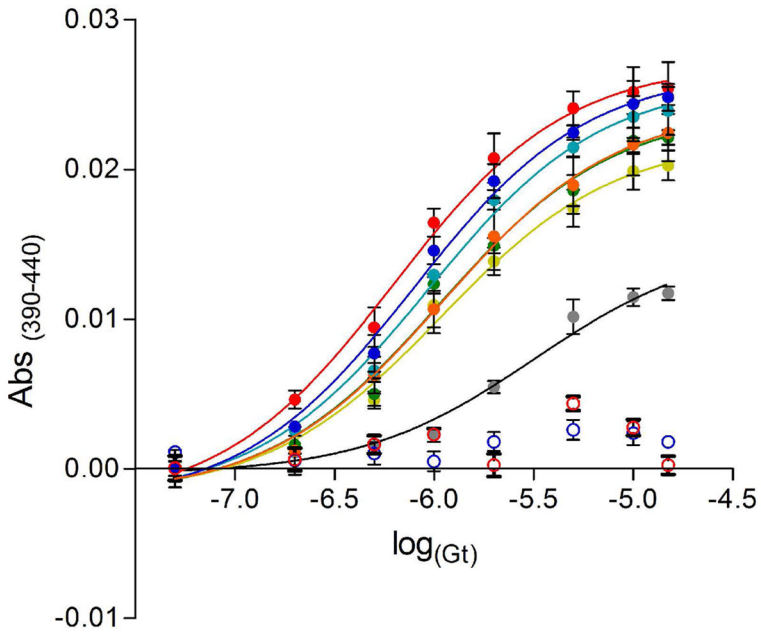

Figure 6.

Effect of negatively charged bicelles on the affinity of G_t for rhodopsin. Concentration-response curves of MII signal stabilized by G_t in the presence of different mixtures of bicelles at a final concentration of 8 % (lipid:rhodopsin ratio of approximately 12800:1). The concentration-response curves were measured at 4 °C and curves are presented for (red) ROS, (empty red circle) ROS + 150 μM GTPγS, (grey) soluble rhodopsin (DDM), (light green) PS (70:30), (green) PS (50:50), (orange) PA (70:30), (light blue) PA+PS (70:30), (dark blue) PA+PS (60:40), (empty dark blue circle) PA+PS (60:40) + 150 μM GTPγS. Solid curves are best fits from a four parameter logistic equation. See Table S2 for estimated EC_{50} values. Results are mean ± S.E.M. from of at least three independent experiments.

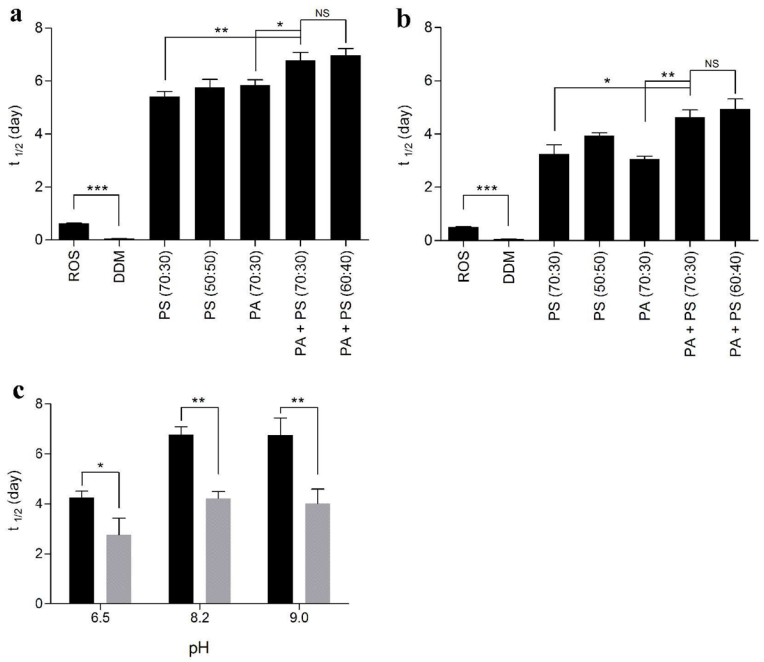

Figure 7.

Stability of rhodopsin-G_t(empty) complex in the presence of negatively charged bicelles. The effect of negatively charged bicelles on complex stability was evaluated at (**a**) 4 °C and (**b**) 15 °C. (**c**) The effect of pH on complex stability at 4 °C (black bars) and at 15 °C (grey bars) in the presence of PA+PS (70:30) bicelles. Final concentrations of PA+PS (70:30) bicelles were held constant at 8% (lipid:rhodopsin ratio of approximately 12800:1). The ratio of neutral to negatively charged phospholipids is indicated within the parentheses in the graph. The half life of extra MII signal was calculated by using an exponential decay equation. Results are mean ± S.E.M. values from at least three independent experiments (* $p < 0.05$; ** $p < 0.01$; *** $p < 0.001$; NS, Not Significant).

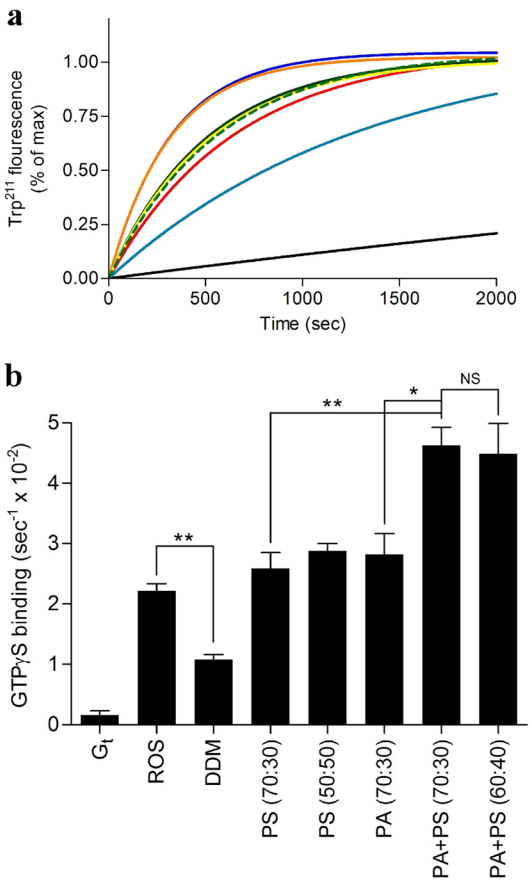

Figure 8.

Intrinsic fluorescence changes in G_t. Basal or receptor mediated nucleotide exchange in G_t was measured in the presence or absence of different bicelles as described in the materials and methods section. Final bicelle concentration in each sample is 8% (lipid:rhodopsin ratio of approximately 12800:1). (**a**) Basal or receptor mediated Trp^{211} fluorescence change of G_t. Fluorescence curves are presented for G_t in the presence of ROS (red), detergent solubilized rhodopsin (DDM) (teal), G_t alone (black), PS (70:30) (green dash), PS (50:50) (green), PA (70:30) (yellow), PA+PS (70:30) (orange), PA+PS (60:40) (blue). Data were collected at 21 °C for 40 min. (**b**) Quantitation of the initial rates of basal or rhodopsin-catalyzed nucleotide exchange for G_t. The ratio of neutral to negatively charged phospholipids is indicated within the parentheses in the graph. Results are mean ± S.E.M. values of at least three independent experiments (* $p < 0.05$; ** $p < 0.01$; NS, Not Significant).